

Free radical polymerization initiated via photoinduced intermolecular electron transfer process: kinetic study 3¹

Janina Kabatc, Zdzisław Kucybała, Marek Pietrzak, Franciszek Ścigalski, Jerzy Pączkowski*

University of Technology and Agriculture, Faculty of Chemical Technology and Engineering, Seminaryjna 3, 85-326 Bydgoszcz, Poland

Received 20 February 1998; revised 6 April 1998

Abstract

Various electron donors and electron acceptors have been tested in order to examine the possibility of the application of the Marcus equation to the description of the kinetics of free radical polymerization photoinitiated via photoinduced electron transfer (PET). Variations of the driving force of the electron transfer, for selected dyes (xanthene dyes, camphorquinone), were introduced by using: a series of tertiary aromatic amines (TAAs) and *N*-phenylglycine derivatives; a series of electron acceptors and only one type of electron donor (cyanine cations with tetraorganylborate anion); a mixed system with a series of benzophenones as electron acceptors and TAAs as electron donors. Several important conclusions follow from the experimental data. (1) For the case with the rate of PET much lower than the rate of diffusion-controlled processes, the Marcus theory can be used for analysing or predicting the ability of organic redox systems for light-induced free radical polymerization. (2) For a process controlled by diffusion, the reactivity of free radicals formed as a result of PET limits the rate of initiation of polymerization. It is shown that this relationship can be also presented as a function of thermodynamic driving forces of the photoredox reaction ($-G^\circ$). For this type of process, the relationship between the rate of polymerization and $-\Delta G^\circ$ is linear, indicating the 'inverted-region-like' kinetic behaviour. Additionally, it is shown that the bleaching process of the dyes competes with the polymerization photoinitiation in a way that suggests that, after free radical formation, two parallel reactions occur and that the rate of bleaching can be expressed as a fraction of the total rate of electron transfer. © 1998 Elsevier Science Ltd. All rights reserved.

Keywords: Photoinitiated free radical polymerization; Dyeing photoinitiators; Photoinduced intermolecular electron transfer

1. Introduction

In the search for systems which undergo a faster and more controllable photopolymerization, the use of visible lasers to initiate and transform, rapidly, a liquid monomer into solid polymer is an important goal. In view of the recent development of dyeing initiating systems active at 488, 514 and 632 nm, both argon-ion and He/Ne lasers are used for such a purpose [1,2]. In commercial practice this type of photoinitiating system is limited to the Mead's Cycolor process² applying the photochemistry of cyanine borates.

Initiation of polymerization via photoinduced intermolecular electron transfer process involves many steps, including photoinduced electron transfer from an electron donor to the singlet or triplet state of the dye followed by secondary reactions, which yield a neutral radical initiating polymerization.

The kinetics of photoinduced intermolecular electron transfer (PET) are usually described using the Marcus theory [3]. However, the practical application of the Marcus theory is commonly used for the study of the primary photochemical processes. The description of the kinetics of the photoinitiated polymerization via intermolecular electron transfer is another example applying this theory to practice [4–6].

The Marcus theory of electron transfer leads to the familiar prediction that the rate of electron transfer first should increase with increase in the thermodynamic driving force $-\Delta G^\ddagger$ and should ultimately decrease with increase of the thermodynamic driving force. This is due to driving forces, ΔG^\ddagger , on the free energy of activation for electron transfer processes [7–12] (for a review on Marcus theory see Ref. [10]).

$$\Delta G^\ddagger = \frac{\lambda}{4} \left(1 + \frac{\Delta G_{el}^\circ}{\lambda} \right)^2 \quad (1)$$

where ΔG^\ddagger is the total free energy of activation and is the

* Corresponding author.

¹ This paper is dedicated to Professor Douglas C. Neckers on the occasion of his 60th birthday.

² Cycolor is a trademark of Mead Corp. The name of process indicates the type of dye used as a primary absorber.

Table 1
Structures of xantheno dyes and their reduction potentials and triplet state energy

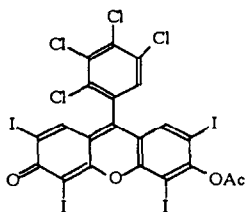
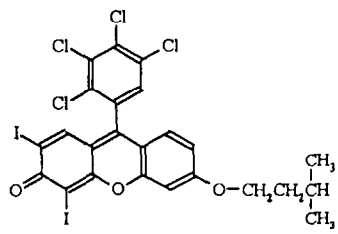
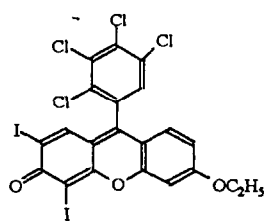
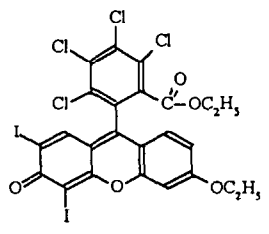
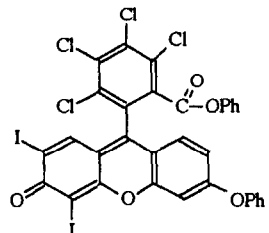
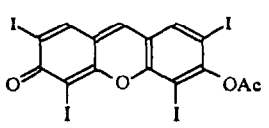
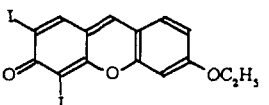
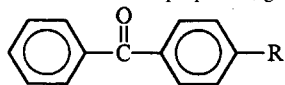
No.	Structure	Abbreviation	$E_{\text{red}}(\text{A}^-/\text{A})$ (V)	E_{00}^{T} (eV)
1		RBAX	-0.80	1.7
2		TDPF	-1.30	2.4
3		TDEF	-1.33	2.4
4		ETDEF	-1.19	2.4
5		BTDBF	-1.09	2.4
6		TIAF	-0.99	1.83
7		DIHF	-0.94	2.3

Table 2
Benzophenones tested and their basic properties; general formula:



No.	R	$E_{\text{red}}(\text{A}^{\cdot-}/\text{A})$ (V)	$E_{\text{oo}}^{(\text{T})}$ (eV) ^a	Hammett constant of R ^a
1	H	-1.550	2.995	0
2	OH	-1.784	2.964	-0.37
3	OMe	-1.676	2.974	-0.27
4	Me	-1.702	2.974	-0.17
5	F	-1.572	3.026	0.06
6	NO ₂	-1.204	2.974	0.78
7	Cl	-1.628	2.985	0.23
8	Ph	-1.540	2.632	-0.01
9	C(O)OEt	-1.630	2.891	0.45
10	COOH	-1.690	2.891	0.45

^a From Ref. [24].

sum of the individual free energies:

$$\Delta G^{\#} = \Delta G_{\text{v}}^{\#} + \Delta G_{\text{s}}^{\#} \quad (2)$$

where the subscripts refer to the energy involving bond distortions of interacting molecules and solvent changes in the ionic sphere surrounding the reactants (s: solvent); λ is defined as the total reorganization energy. Thus, $\lambda = \lambda_{\text{v}} + \lambda_{\text{s}}$, where λ_{v} is the inner-sphere reorganization energy referring to the energy changes of the molecule geometry during the electron transfer step, and λ_{s} is the outer-sphere reorganization energy which is caused by the energy change as the solvent shell surrounding the reactants rearranges. Finally, $\Delta G_{\text{el}}^{\circ}$ is expressed by the Rehm–Weller [13,14] equation:

$$\Delta G_{\text{el}}^{\circ} = E_{\text{ox}}(\text{D}/\text{D}^{\cdot+}) - E_{\text{red}}(\text{A}^{\cdot-}/\text{A}) - Ze^2/\epsilon a - E_{\text{oo}} \quad (3)$$

where $E_{\text{ox}}(\text{D}/\text{D}^{\cdot+})$ is the oxidation potential of the electron donor, $E_{\text{red}}(\text{A}^{\cdot-}/\text{A})$ is the reduction potential of the electron acceptor, E_{oo} is the energy of the excited state and $Ze^2/\epsilon a$ is the Coulombic energy which is considered negligible compared with the overall magnitude of ΔG in the present systems.

In our earlier papers [4–6] we have shown that the Marcus equation can be applied for the description of the kinetics for a dye-photoinitiated polymerization via an intermolecular electron transfer process. In this paper it is our intention to extend the kinetic considerations for a wider range of dyes and electron donors and to illustrate the possibility of adaptation of the Marcus theory for description of the kinetics of photopolymerization sensitized by the dyes.

2. Experimental section

2.1. Dyeing initiators

(1) RBAX: the Rose Bengal derivative was prepared from Rose Bengal according to the procedure described by Neckers and coworkers [15]. Its reduction potential is assumed to

be equal to the reduction potential of Rose Bengal C2' benzyl ester, sodium salt [16], e.g. $E_{\text{red}}(\text{A}^{\cdot-}/\text{A}) = -0.80$ V and its triplet $E_{\text{oo}} = 1.7$ eV [17,18].

(2) TDEF (3',4',5',6'-tetrachloro-5,7-diiodo-3-ethoxy-6-fluorone), TDPF (3',4',5',6'-tetrachloro-5,7-diiodo-3-(3-methylbutoxy)-6-fluorone), ETDEF (2'-ethoxycarbonyl-3',4',5',6'-tetrachloro-5,7-diiodo-3-ethoxy-6-fluorone) and BTDBF (2'-benzyloxycarbonyl-3',4',5',6'-tetrachloro-5,7-diiodo-3-benzyloxy-6-fluorone) were prepared by the method based on the modified chemistry of xanthenes described by Neckers and coworkers [19–21].

(3) TIHF, tetraiodohydrofluorescein (2,4,5,7-tetraiodo-6-hydroxyfluorone), was synthesized according to the method of Shi and Neckers (see Refs. [35,36]). Its reduction potential and triplet state energy according to Rodgers and Neckers are $E_{\text{red}}(\text{A}^{\cdot-}/\text{A}) = -0.99$ V (versus SCE), (our measurement $E_{\text{red}}(\text{A}^{\cdot-}/\text{A}) = -0.940$ V (versus 1 M Ag–AgCl) and $E_{\text{oo}}^{(\text{T})} = 1.83$ eV (42.3 kcal mol⁻¹). For photopolymerization experiments TIHF was acetylated using a similar procedure as for RBAX [15].

(4) DIHF, diiodohydrofluorescein (3-alkoxy-5,7-diiodo-6-fluorone), was synthesized according to the method of Shi and Neckers (see Ref. [22]). Its reduction potential measured using cyclic voltammetry is $E_{\text{red}}(\text{A}^{\cdot-}/\text{A}) = -0.94$ V and $E_{\text{oo}}^{(\text{T})} = 2.3$ eV [23].

The structures of the xanthene dyes tested and their reduction potentials and energies of triplet states are summarized in Table 1.

(5) Camphorquinone (CQ) was purchased from Aldrich. Its reduction potential is $E_{\text{red}}(\text{A}^{\cdot-}/\text{A}) = -1.249$ V and $E_{\text{oo}}^{(\text{T})} = 51$ kcal mol⁻¹ [24].

(6) Benzophenones were purchased from Aldrich. Their reduction potentials were measured using cyclic voltammetry and are presented in Table 2.

(7) Cyanine borates were prepared in our laboratory. The method of synthesis and their spectroscopic and photochemical properties have been described elsewhere [25].

2.2. The electron donors

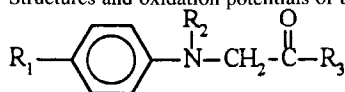
(1) The tertiary aromatic amines (TAAs) are described in an earlier paper [5].

(2) *N*-Phenylglycine derivatives (NPGs) were prepared by published procedures [26–29] and are listed in Table 3.

The oxidation and reduction potentials were measured using cyclic voltammetry. For measurements, an Electroanalytical Cypress System Model CS-1090 was used and an AgCl electrode served as a reference electrode. The supporting electrolyte was 0.1 M tetrabutylammonium perchlorate (TBAP).

The kinetics of free radical polymerization were studied using either a polymerization solution composed of 1 ml of MP and 9 ml of 2-ethyl-2-(hydroxymethyl)-1,3-propanediol triacrylate (TMPTA) or 10 ml of TMPTA. Dye concentration was 5×10^{-4} M and the electron donor concentration was 0.1 M.

Table 3
Structures and oxidation potentials of tested electron donors with general formula



No.	N-substituent R ₂	<i>p</i> - (<i>-o</i> , <i>-m</i>) substituent R ₁	R ₃	E _{ox} (mV)
1	H	H	OH	426
2	H	NC	OH	707
3	H	NO ₂	OH	781
4	H		OH	635
5	H		OH	661
6	H		OH	639
7	H	Cl	OH	479
8	H	CH ₃	OH	437
9	H	<i>tert</i> -But.	OH	436
10	H	PhO	OH	479
11	H	MeO	OH	343
12	Me	H	OH	—
13		H	OH	2000
14	H	H	OEt	1080
15	H	CN	OEt	1642
16	H	NO ₂	OEt	1598
17	H		OEt	1352
18	H		OEt	1340
19	H	Me	OEt	1010
20	H	<i>p</i> -Cl	OEt	1132
21	H	<i>o</i> -Cl	OEt	1266
22	H	<i>m</i> -Cl	OEt	1244
23	H	OMe	OEt	862
24	H	H	NH ₂	984
25	Ph	H	OEt	1064

Measurements were performed in a home-made micro-calorimeter. As a temperature sensor a semiconducting diode immersed in the 2 mm thick layer (0.25 ml) of a cured sample was used. The amplified signal was transformed with an analog/digital data acquisition board to a computer. Irradiation of the polymerization mixture was carried out using the emission of an Omnicrome argon ion laser Model 543-500MA with intensity of light of 30 mW/0.785 cm². An average value of the rate of polymerization was established based on measurements performed at least three times. The light intensity was measured by a Coherent power meter Model Fieldmaster. For benzophenones sensitized photopolymerization, irradiation of the polymerization mixture was carried out using part of the UV emission (300–400 nm) of a xenon lamp (Philips CSX 150 W/1) with intensity of irradiation $I = 120 \text{ mW/cm}^2$. The light intensity was measured by an IL 1400A Int. Light Inc. (USA) radiometer.

The second method is based on real-time i.r. spectroscopy (RTIR) [30–32] and allowed the rate of monomer double bond disappearance to be monitored in real time. By following the disappearance of the i.r. absorption of the acrylic double bond, one can quantitatively evaluate the rate of polymerization. The i.r. spectrometer (Specord-IR 71, Carl-Zeiss Jena) was set in the transmission mode and the detection wavelength fixed at a value where the monomer double bond exhibits a discrete and intense absorption, e.g. at 810 cm⁻¹ for acrylic monomers (–CH=CH₂ twisting). The signal was transformed with an analog/digital data acquisition board to a computer. A thin film (transmittance at 810 cm⁻¹ in a range of 90%) coated onto polyethylene sheet, placed between NaCl salt discs, was irradiated by an Omnicrome argon-ion laser Model 543-500 MA with intensity of light of 200 mW/0.785 cm². Measurements for each electron donor were made at least three times.

All calculations were made using Microsoft Excel 4 software. Graphs and calculations of fittings and calculations of statistical fitting parameters were performed using Side-Write Plus 2 software.

3. Results and discussion

The process of free radical initiated polymerization via the intermolecular electron transfer process involves many steps which are dependent on the nature of the dye and the electron donor. For tertiary aromatic amines, they include an electron transfer between an excited acceptor (A) and an electron donor (D) followed by a proton transfer from the electron donor radical cation to the dye radical anion [33,34], which yields a neutral radical initiating polymerization and the reduced radical of the dye. Initiation of polymerization for cyanine dye–tetraorganylborate salt involves alkyl radical formation as a result of photoinduced electron transfer from borate anion to the singlet state of the cyanine cation [1,2]. In the intimate ion pair, the cyanine dye in its excited singlet state oxidized the borate anion by electron transfer and the boranyl radical cation decomposes forming a radical which initiates polymerization. The process involved a short-lived excited singlet state; therefore, the initiation abilities of cyanine dyes are much lower than the photoreactivity of xanthenes dyes studied by Necker's group [35,36,22]. The use of NPGs as electron donors gives even more complex processes following electron transfer, yielding free radicals as a result of *N*-phenylglycine cation radical decomposition [37]. Also very complex is the photochemistry of the dye–sulfur-containing amino-acid photoinitiation pair [38–41].

The cross-coupling between radical pairs of donor–acceptors terminates the photoreaction [42]. The cross-coupling between radicals competes with initiation of free radical polymerization. Additionally, one should mention that if the reaction takes place within the solvent cage, the products that are formed may revert back to starting reactants or leave the solvent cage by ion dissociation.

It was shown in our earlier paper [6] that in solid or very viscous media (diffusionless electron transfer) the rate of photoinitiated polymerization can be described by the equation

$$R_p = -\frac{d[M]}{dt} = k_p[M] \sqrt{\frac{I_a K_a}{k_t}} \times \sqrt{\chi Z \exp\left[-\frac{\lambda}{4} \left(1 + \frac{\Delta G^\circ}{\lambda}\right)^2\right] - k_{bl}[D \cdots A \cdot H]} \quad (4)$$

or, when cross-coupling between free radicals formed can

be neglected, by the expression

$$R_p = -\frac{d[M]}{dt} = k_p[M] \sqrt{\frac{I_a K_a}{k_t}} \chi Z \exp\left[-\frac{\lambda}{4} \left(1 + \frac{\Delta G^\circ}{\lambda}\right)^2\right] \quad (5)$$

Eq. (5) can be also expressed in logarithmic form

$$\ln R_p = A - \frac{\lambda}{4} \left(1 + \frac{\Delta G^\circ}{\lambda}\right)^2 \frac{1}{RT} \quad (6)$$

where *A* combines all constant data for the start of polymerization.

Experimental verification of the use of Marcus theory for the description of photoinitiated polymerization needs a wide range of experiments. Therefore, only an equation describing the rate of polymerization in viscous monomeric system was tested using well-known electron acceptors and electron donors.

Examples of the kinetic curves of photopolymerization recorded in real time are presented in Fig. 1.

In order to reduce the effect of diffusion-controlled termination [43–47], the effect of network formation and the Norrish–Troomsdorf effect, the initial rates of polymerization were taken into account for further consideration (initial rates of polymerization are slopes of the lines drawn on the flow of heat versus time curves at initial time of polymerization). Fig. 2 presents the relationship for polymerization rate (arbitrary units) of TMPTA versus ΔG° using RBAX–TAAs initiating pairs. The properties of RBAX–NPGs initiating pairs are illustrated in Fig. 3.

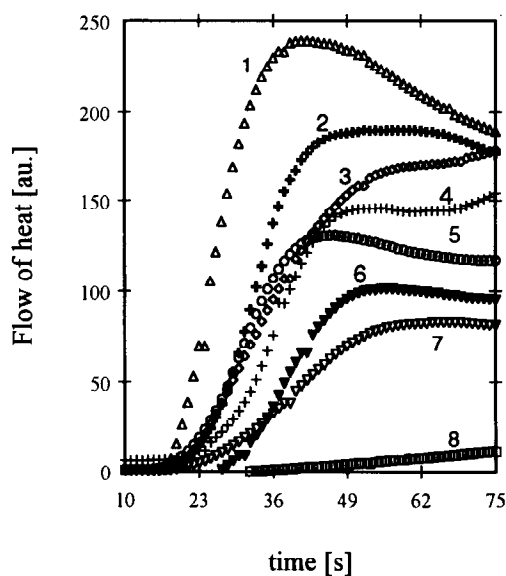


Fig. 1. The family of curves recorded during the measurements of the flow of heat during photoinitiated polymerization of TMPTA initiated by benzophenones–4-bromo-*N,N*-dimethylaniline initiating photoredox pairs. Type of benzophenone: (1) 4-Ph, (2) 4-C(O)OEt, (3) 4-Me, (4) 4-H, (5) 4-Cl, (6) 4-F, (7) 4-OMe, (8) 4-NO₂.

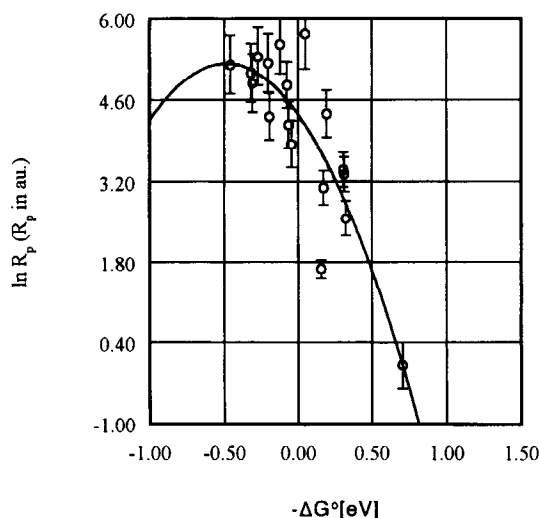


Fig. 2. The Marcus plot of rates of polymerization (au) of TMPTA-MP (9:1) mixture for the RBAX-TAAS initiating system. The parabola fitting curve gives $R^2 = 0.91$.

The experimental results presented in Figs 2 and 3 suggest that the intermolecular electron transfer process might be the limiting step in the photoinitiated polymerization. Data show that the rate of polymerization is reduced when the thermodynamic driving force ($-\Delta G^\circ$) is increased, so demonstrating the 'inverted-region-like' kinetic behaviour. The experimental results shown in Fig. 2 can be fitted to the shape of part of a parabola or can be presented as a linear relationship (Fig. 4).

Neckers and coworkers [48] established that for Rose Bengal derivatives the rates of triplet quenching by aromatic amines range between 10^9 and $10^{10} \text{ M}^{-1} \text{ s}^{-1}$, i.e. are close to the rate constant calculated for diffusion-controlled reaction. This observation allows us to conclude that, for RBAX-TAAs initiating pairs, the rate of the intermolecular electron transfer is not the limiting step for the entire

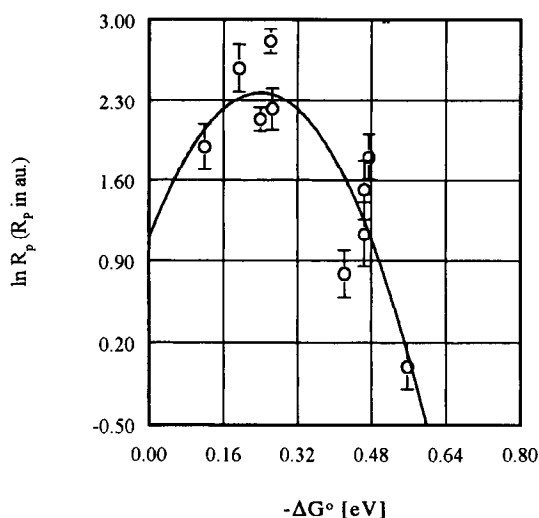


Fig. 3. The Marcus plot of rates of polymerization (au) of TMPTA-MP (9:1) mixture for the RBAX-NPGs initiating system. The parabola fitting curve gives $R^2 = 0.87$.

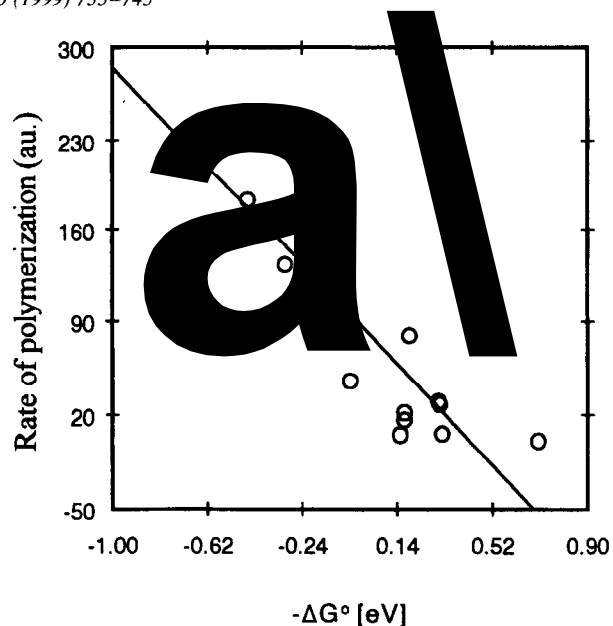


Fig. 4. Relationship between the rate of polymerization of TMPTA-MP (9:1) mixture and the free energy of activation for photoredox reaction for the RBAX-TAAs initiating system. The linear fitting gives for experimental points $R^2 = 0.87$.

process. Assuming that the intermolecular electron transfer for the tested system is diffusion-controlled, i.e. independent, as an explanation of the existence of the 'inverted-region-like' behaviour one can assume variation of the reactivity of free radicals formed as a result of processes occurring after electron transfer. Variation of the free radical reactivity can be explained as a substituent effect on the rate of initiation of the polymerization chain. Mateo et al.

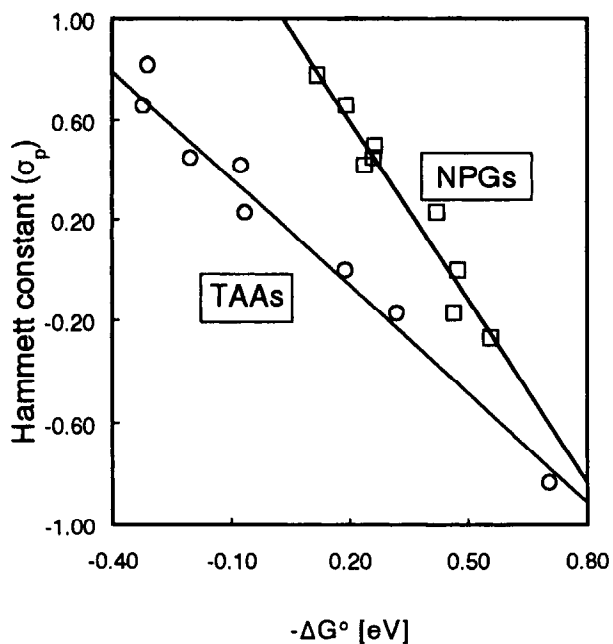


Fig. 5. Relationship between the Hammett constant and the photoredox properties of the photoinitiating system (RBAX-TAAs and RBAX-NPGs) described by the Rehm-Weller equation. The linear fitting gives for experimental points: (A) $R^2 = 0.97$ and (B) $R^2 = 0.99$.

[49] have shown that the relative reactivity of radicals derived from dimethylanilines increases as the Hammett parameter σ_p increases. The relationship between and Hammett constant σ_p for the electron donors tested is presented in Fig. 5. The results clearly show a linear relationship. Assuming

$$R_p = \rho \sigma_p \quad (7)$$

and

$$-\Delta G^\circ = \rho' \sigma_p \quad (8)$$

combination of Eqs. (7) and (8) gives

$$R_p = \frac{\rho}{\rho'} (-\Delta G^\circ) \quad (9)$$

The final equation clearly shows the linear relationship between the rate of polymerization and the Hammett constant and this is illustrated in Fig. 4. This behaviour is also supported by results obtained for camphorquinone–NPGs (Fig. 6), tested as an initiating system for 3D and dental applications.

More interesting is the behaviour of a new group of xanthene dyes used for photoinitiation of free radical polymerization [35,36,22,23]. The laser flash photolysis studies performed for novel xanthene dyes [33,34] have shown that the rates of triplet state quenching of iodohydrofluoresceins by aromatic amines are in the order of $2.4 \times 10^7 \text{ M}^{-1} \text{ s}^{-1}$ for tetraiodohydrofluorescein [23] (2,4,5,7-tetraiodo-3-hydroxy-6-fluorone, TIHF) and $1.21 \times 10^8 \text{ M}^{-1} \text{ s}^{-1}$ for 5,7-diiido-3-butoxy-6-fluorone (DIBF). Both rates of electron transfer are below the rate of diffusion-controlled reaction. Results for rates of polymerization for the TIAF–NPGs system are presented in Fig. 7.

Here, important differences can be seen in the shapes of curves describing the relationship $R_p = f(-\Delta G^\circ)$. It is clear

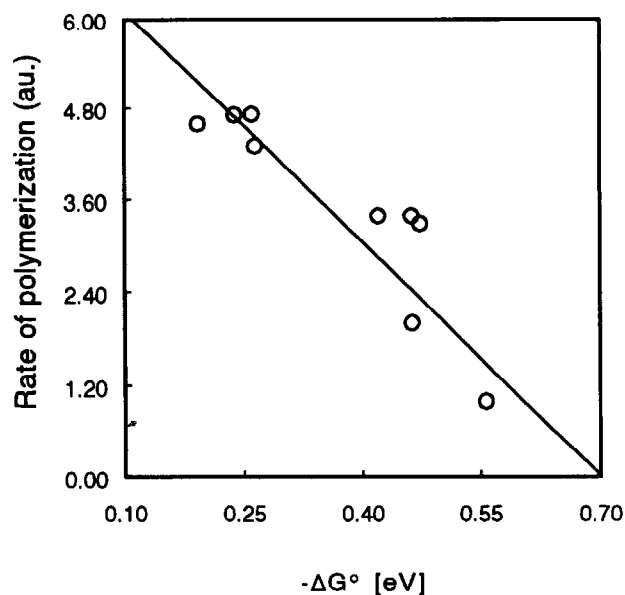


Fig. 6. Relationship between the rate of polymerization and the free energy of activation for photoredox reaction for the camphorquinone–NPGs initiating system. The linear fitting gives for experimental points $R^2 = 0.95$.

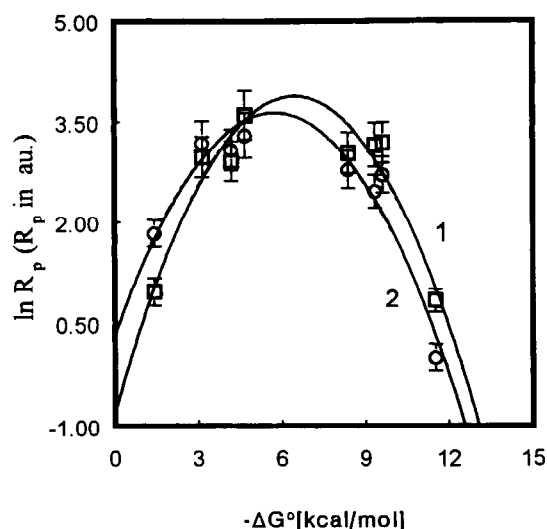


Fig. 7. The Marcus plot of the rates of polymerization (au) of: (1) TMPTA–MP (10:4); (2) TMPTA–MP–THF (14:1:6) for the TIAF–NPGs initiating system. The curves fitted to the Marcus equation give for: (1) $\lambda = -6.49 \text{ kcal mol}^{-1}$, $R^2 = 0.91$; (2) $\lambda = -5.78 \text{ kcal mol}^{-1}$, $R^2 = 0.92$.

that a change of the acceptor type causes significant variation in the kinetics of photoinitiated polymerization. The fitting obtained for the TIAF–NPGs initiating system gives a full parabola, whereas for RBAX–NPGs one observes only a part of this curve. Since for both initiating systems, i.e. RBAX–NPGs and TIAF–NPGs, the resulting free radicals are identical, this deviation cannot be explained by reactivity of the free radicals resulting from the secondary processes occurring after photoinduced electron transfer. The TIAF–TAAs (Fig. 8) initiating systems behave similarly. Fig. 6 illustrates the linear relationship between the rate of polymerization and the Hammett constant for the camphorquinone–NPGs initiating system. The study of

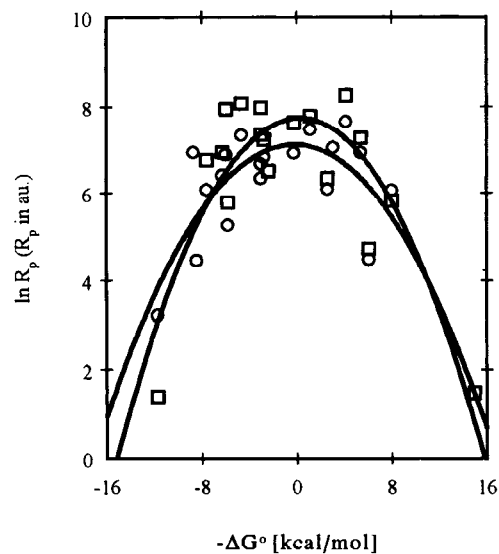


Fig. 8. Marcus plot of the rate of polymerization (au) initiated by TIAF–TAAs initiating system; squares: TMPTA–MP (10:4) mixture; circles: TMPTA–THF mixture (10:4).

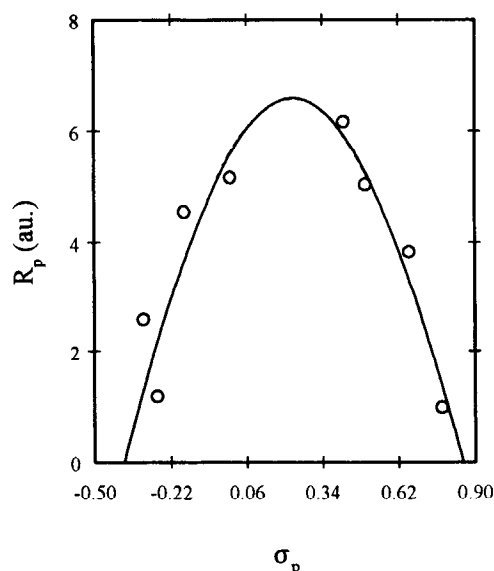


Fig. 9. Relationship between the rate of polymerization (TMPTA-MP) and the Hammett constants for photoredox reaction for the DIHF-NPGs initiating system:

DIHF-NPGs initiating pairs shows quite different behaviour. For essentially the same free radicals formed (radicals resulting from NPGs), one observes data suggesting that, for the DIHF-NPGs initiating system, the reactivity of the free radicals formed does not affect the rate of polymerization (see Fig. 9). The type of relationship observed indicates that the rate of photoinduced intermolecular electron transfer is more likely to be the limiting step of the process.

In our earlier papers, the study of the kinetics of photoinitiated polymerization was limited to a few photoredox pairs, covering a relatively narrow range of ΔG° . For better verification, more electron donors from the *N*-phenylglycine family have been synthesized and tested, using xanthene dyes as electron acceptors. Fig. 10 shows the

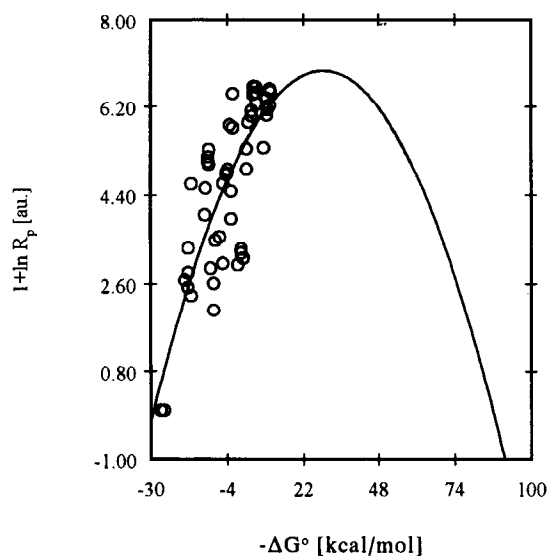


Fig. 10. Marcus plot of the rate of polymerization (TMPTA-MP) initiated by two different initiating systems: DIHF-NPGs and TIAF-NPGs.

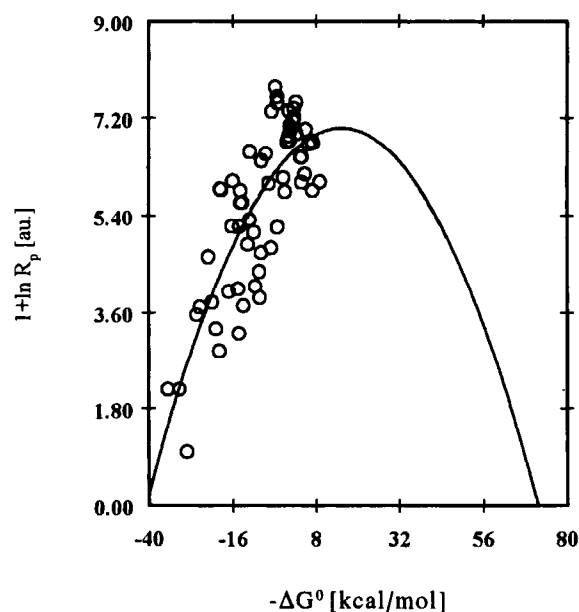


Fig. 11. Marcus plot of the rate of polymerization (TMPTA-MP) initiated by four different initiating systems: TDEF-NPGs, ETDEF-NPGs, TDPF-NPGs and BTDBF-NPGs.

Marcus plot obtained for two different dyes (DIHF and TIAF) and NPGs.

The results clearly show that the experimental points obtained for the TIAF and DIHF as the electron acceptors and NPGs can be fitted to the shape of parabola (part), with experimental data being in the normal Marcus region. Similar properties are observed for Rose Bengal derivatives used as electron acceptors (Fig. 11).

Visible initiators often bleach, as they generate reaction intermediates. The photoreduction of dyes, in the absence of monomers, should also show characteristics indicating the link between the rate of photoinduced intermolecular

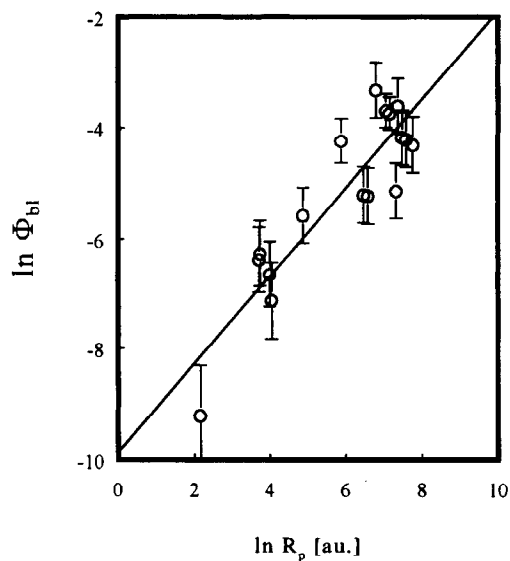


Fig. 12. Relationship between the rate of polymerization (TMPTA-MP) and quantum yield of photobleaching process for TDEF-NPGs and ETDEF-NPGs photoredox pairs.

electron transfer and the quantum yield of the bleaching process. For Rose Bengal derivatives and NPGs, this is shown in Fig. 12.

From Fig. 12, it is evident that the rate of the bleaching process can also be described using the Marcus relationship. According to the general kinetic scheme for polymerization photoinduced by xanthene dyes in the presence of TAAAs [5,6,34], the colourless products obtained during the polymerization originate from two different reactions. The first, involves reactions following the electron transfer, i.e. a proton transfer and then the radical anion formed abstracts hydrogen either from the electron donor or from the solvent (monomer). This process does not compete with photoinitiation of polymerization. The second path involves the cross-coupling reaction between the free radicals formed from both an electron acceptor and an electron donor [50]. The above-mentioned reaction strongly decreases the efficiency of free radical photopolymerization (see Eq. (4)).

Kinetic analysis of the photobleaching in an inert solvent indicates that, for a given dye, the rate of bleaching is directly proportional to the quantum yield of the process. Fig. 12 shows the relationship between the rate of polymerization and the quantum yield of the bleaching process. It is obviously a linear relation ($R^2 = 0.93$). This indicates that the formation of free radicals is followed by two parallel reactions, and that the rate of bleaching can be expressed as a fraction of the total rate of electron transfer:

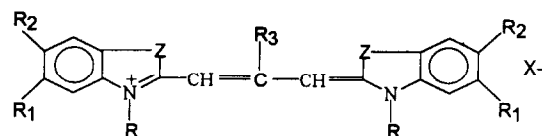
$$R_p = -\frac{d[M]}{dt} = k_p[M] \sqrt{\frac{I_a K_a}{k_t}} \sqrt{\chi Z \exp\left[-\frac{\lambda}{4} \left(1 + \frac{\Delta G^\circ}{\lambda}\right)^2\right] - K \exp\left[-\frac{\lambda}{4} \left(1 + \frac{\Delta G^\circ}{\lambda}\right)^2\right]} \quad (10)$$

where K is the fraction of electron transfer process used for photobleaching. The final equation, after this simplification, becomes less complex and can be expressed as

$$R_p = -\frac{d[M]}{dt} = k_p[M] \sqrt{\frac{I_a K_a}{k_t}} \sqrt{\xi \exp\left[-\frac{\lambda}{4} \left(1 + \frac{\Delta G^\circ}{\lambda}\right)^2\right]} \quad (11)$$

where ξ is a combined constant containing χ , Z and K . From Eq. (11) one can deduce that, for selected groups of photoredox pairs which form bleached products via a free radical cross-coupling reaction, the rate of polymerization can be presented in a form similar to that describing the rate of polymerization without the bleaching reaction.

For the photoinitiating systems described above, variation of the driving force of the electron transfer process was brought about by using a series of tertiary aromatic amines or by using a series of NPGs. These types of photoredox pairs produce different types of free radicals, which



Scheme 1.

can also have an effect on the final experimental results, even for k_{el} much lower than the diffusion limit. A different approach to change of the driving force of electron transfer is possible by applying various electron acceptors, while the electron donor remains unvaried. Such a possibility leads to the dyeing photoinitiators described by Gottschalk and coworkers [1,2] who applied the photochemistry of cyanine borates.

The structures of the cyanine borates tested are presented in Scheme 1. Here X^- is $[(Ph)_3BuB]$ anion. By changing Z , R , R_1 , R_2 and R_3 , the reduction potentials of the dyes were modified [25]. Fig. 13 presents the Marcus plot obtained for the photopolymerization rates when using cyanine–borate photoredox pairs.

The results clearly show that the change of the acceptor type, without a change of the donor, gives the relationship described by Eq. (5), i.e. the equation predicting that the rate of polymerization is in part controlled by the rate of

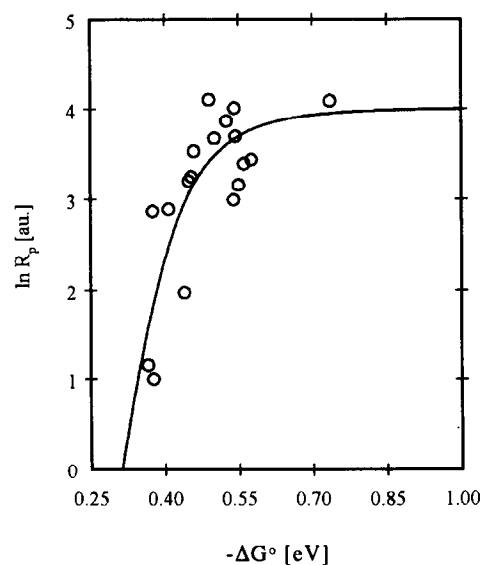


Fig. 13. Marcus plot obtained for the rates of photopolymerization (TMPTA–MP) using cyanine–borate photoredox pairs.

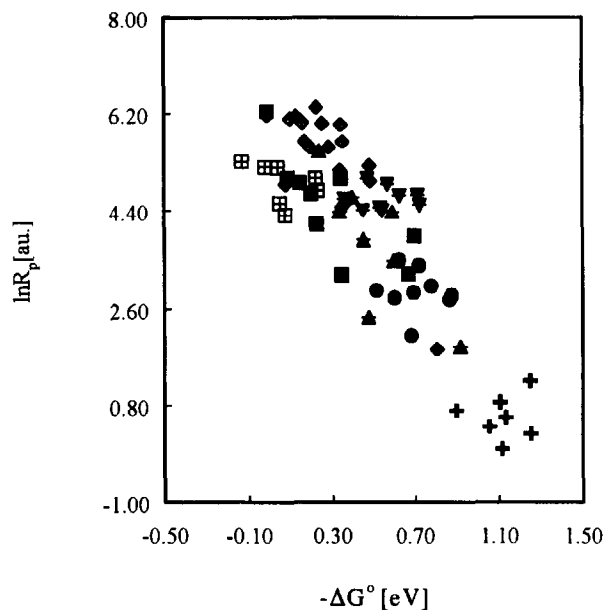


Fig. 14. Relationship between the rate of polymerization (TMPTA) and the free energy of activation for photoredox reaction for benzophenones–TAAs initiating systems.

photoinduced electron transfer. As a consequence, the Marcus equation can be applied for the description of the rate of the polymerization photoinitiated via photoinduced intermolecular electron transfer. The relationship presented in Fig. 13 shows typical ‘normal Marcus region’ kinetic behaviour.

One more initiating system was tested in order to verify the adaptation of the Marcus equation for description of the kinetics of the photoinitiated polymerization. Fig. 14 shows

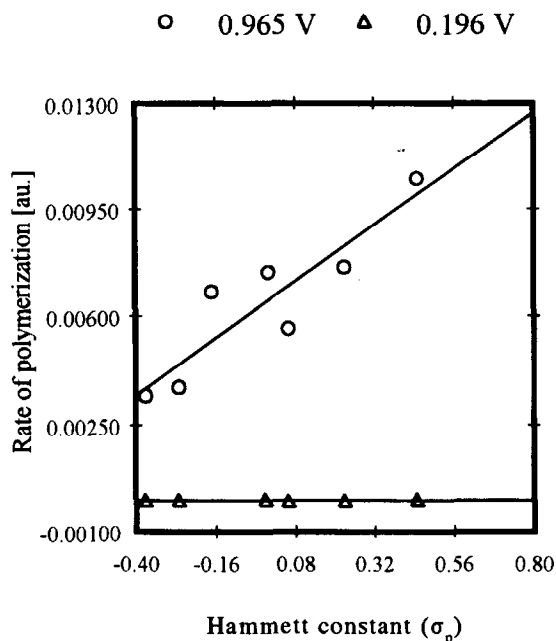


Fig. 15. Relationship between the rate of photoinitiated polymerization (TMPTA) and the Hammett constants for benzophenones tested and the oxidation potential values of TAAs tested.

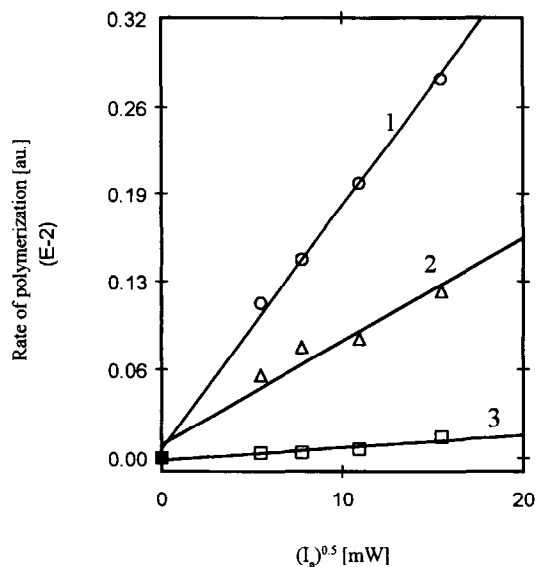


Fig. 16. Rate of polymerization versus light intensity for the cyanine–borate initiating system. Cyanine dye (see Scheme 1): Z = S, R1 = R2 = R3 = H, R = Et, concentration of photoinitiator: (1) 1×10^{-3} M, (2) 1×10^{-4} M, (3) 5×10^{-5} M.

the rates of polymerization as a function of free energy of activation for a series of benzophenones used as electron acceptors and a series of TAAs used as electron donors.

Data presented in Fig. 14 show that the rates of polymerization become less when the thermodynamic driving force ($-\Delta G^\circ$) is increased, demonstrating ‘inverted-region-like’ kinetic behaviour. There are at least two explanations for these specific properties. The first is that, for the benzophenone–TAAs initiating systems, there is no electron transfer between the excited acceptors and donors and that the free radicals are formed as a result of hydrogen abstraction from an electron donor by the benzophenone triplet state. The second possibility is that the reactivity of the ketyl radicals resulting from electron transfer is a function of Hammett parameter σ_p . Thus the recombination process between the ketyl radical and a radical derived from an electron donor is controlled by the reactivity of both radicals. These possibilities are illustrated in Fig. 15. On the basis of results shown in Fig. 15, it appears that the second explanation is acceptable for this specific behaviour.

Eqs. (4), (5) and (11) predict that for an identical photoredox initiating pair one should observe demonstration of the ‘normal polymerization kinetics’, i.e. the rate of polymerization should increase linearly with the square-root of the light intensity. Data presented in Fig. 16 illustrate this prediction.

Photopolymerization initiated by cyanine–borate photoredox pairs, as is shown in Fig. 16, proceeds by the conventional mechanism in which bimolecular termination occurs by reaction between two macroradicals. This suggests that free radicals formed from cyanine ion after a photoinduced electron transfer process do not act as terminators of polymer chains.

Acknowledgements

This research was sponsored by the State Committee for Scientific Research (KBN), grants BS-7/93, BW-21/93 and No 3 T09A 012 11.

References

- [1] Chatterjee S, Gottschalk P, Davis PD, Schuster GB. *J Am Chem Soc* 1988;110:2326.
- [2] Chatterjee S, Davis PD, Gottschalk P, Kurz ME, Saverwien B, Yang X, Schuster GB. *J Am Chem Soc* 1990;112:6329.
- [3] Marcus RA. *Annu Rev Phys Chem* 1964;15:155.
- [4] Kucybała Z, Pietrzak M, Pączkowski J, Lindn L-A, Rabek JF. *Polymer* 1996;37:4585.
- [5] Pączkowski J, Kucybała Z. *Macromolecules* 1995;28:269.
- [6] Pączkowski J, Pietrzak M, Kucybała Z. *Macromolecules* 1996;29:5057.
- [7] Marcus RA. *J Chem Phys* 1956;24:966.
- [8] Marcus RA. *J Chem Phys* 1963;67:853.
- [9] Marcus RA. *J Chem Phys* 1965;43:679.
- [10] Kavarnos GJ. Photoinduced electron transfer I. *Topics in Current Chemistry* 1990;156:21.
- [11] Suppan P. Photoinduced electron transfer IV. *Topics in Current Chemistry* 1992;163:95.
- [12] Ebersson L. *Electron transfer in organic chemistry*. New York: Springer, 1987.
- [13] Rehm D, Weller A. *Ber Bunsenges Phys Chem* 1969;73:834.
- [14] Rehm D, Weller A. *Isr J Chem* 1970;8:259.
- [15] Valdes-Aquilera O, Pathak CP, Shi J, Watson D, Neckers DC. *Macromolecules* 1992;25:541.
- [16] Linden SM, Neckers DC. *J Am Chem Soc* 1988;110:1257.
- [17] Pączkowski J, Lamberts JJM, Pączkowska B, Neckers DC. *J Free Radicals Biol Med* 1985;7:341.
- [18] Neckers DC. *Photochem Photobiol A: Chem* 1989;47:1.
- [19] Lamberts JJM, Neckers DC. *Z Naturforsch Teil B: Chem* 1984;39:474.
- [20] Lamberts JJM, Schumacher DR, Neckers DC. *J Am Chem Soc* 1984;106:5879.
- [21] Pietrzak M, Pączkowski J, submitted to *Polimery*.
- [22] Tanabe T, Torres-Filho A, Neckers DC. *J Polym Sci Part A: Polym Chem* 1995;33:1691.
- [23] Hassoon S, Neckers DC. *J Org Chem* 1995;99:9416.
- [24] Murov SL, Carmichael I, Hug GL. *Handbook of photochemistry*, 2nd edn. New York: Marcel Dekker, 1993.
- [25] Kabatc N, Pietrzak M, Pączkowski J, submitted to *Macromolecules*.
- [26] Knoevenagel E *Berichte* 1904;37:4065.
- [27] Schwalbe CG, Schulz W, Jochheim. *Berichte* (1908) 41, 3790.
- [28] Trophe JE, Wood AS. *J Chem Soc* 1913;103:1601.
- [29] Bischoff CA, Hausdrfer A. *Berichte* 1892;25:2345.
- [30] Decker C, Moussa K. *Makromol Chem* 1988;189:2381.
- [31] Decker C, Moussa K. *Macromolecules* 1989;22:4455.
- [32] Decker C, Moussa K. *ACS Symp. Ser.* 1990;417:439. (and references cited therein).
- [33] Klimtchuk E, Rodgers MAJ, Neckers DC. *J Phys Chem* 1992;96:9817.
- [34] Hassoon S, Neckers DC. *J Phys Chem* 1995;99:9416.
- [35] Shi J, Zhang X, Neckers DC. *J Org Chem* 1992;57:4418.
- [36] Shi J, Zhang X, Neckers DC. *Tetrahedron Lett* 1993;34:6013.
- [37] Kucybała Z, unpublished data.
- [38] Bobrowski K, Marciniak K, Hug GL. *J Photochem Photobiol A: Chem* 1994;81:159.
- [39] Marciniak B, Bobrowski K, Hug GL, Rozwadowski J. *J Phys Chem* 1994;98:4854.
- [40] Marciniak B, Hug GL, Bobrowski K, Kozubek H. *J Phys Chem* 1994;98:537.
- [41] Marciniak B, Hug GL, Bobrowski K, Kozubek H. *J Phys Chem* 1995;98:13560.
- [42] Pandey G Photoinduced electron transfer V. *Topics in Current Chemistry* 1993;168:175.
- [43] Anseth KS, Wang CM, Bowman CN. *Macromolecules* 1994;27:650.
- [44] Pączkowska B, Pączkowski J, Neckers DC. *Polimery* 1994;39:527.
- [45] Anseth KS, Wang CM, Bowman CN. *Polymer* 1994;35:3243.
- [46] Kurdikar DL, Peppas NA. *Macromolecules* 1994;27:4084.
- [47] Andrzejewska E, Bogacki MB. *Macromol Chem Phys* 1997;198:1649.
- [48] Witteges V, Scaiano JM, Linden SM, Neckers DC. *J Org Chem* 1989;54:5242.
- [49] Mateo JL, Bosh P, Lozano AE. *Macromolecules* 1994;27:7794.
- [50] Philips K, Read G. *J Chem Soc Perkin Trans* 1986;1:671.